

# Use of Body Model Constraints to Improve Accuracy of Inertial Motion Capture

A. D. Young

Institute for Computing Systems Architecture  
School of Informatics, University of Edinburgh  
10 Crichton Street Edinburgh EH8 9AB, United Kingdom  
Email: ayoung9@inf.ed.ac.uk

**Abstract**—Presents simulations of an algorithm for estimating linear acceleration of wireless inertial measurement units based on body model constraints. The behaviour of the proposed algorithm is compared to existing algorithms based on motion capture data from the Carnegie Mellon University motion capture corpus.

The new algorithm is demonstrated to be capable of accurately estimating linear accelerations for walking and running motions. The use of linear acceleration estimation is demonstrated to improve the accuracy of inertial motion capture.

## I. INTRODUCTION

The use of wireless Inertial Measurement Units (IMUs) has become increasingly common as low-cost, low-power, inertial sensors, such as accelerometers and rate gyroscopes, have become available. Two major application areas have emerged: activity monitoring and automated motion classification [1]–[5], and motion capture [6]–[10].

Activity monitoring and classification applications generally attempt to use a small number of sensors, in order to reduce cost and inconvenience to the subject, placed to achieve the maximum differentiation between the activities of interest. In contrast, systems designed to track the relative rotations of the subject's joints use numerous sensors to track the orientations of the subject's limb segments.

In contrast to traditional methods of motion capture, such as optical and magnetic trackers which have a limited tracking volume, wireless inertial systems allow for motion capture with little limitation to subject position. Furthermore, wireless sensors are less cumbersome to the subject than older mechanical tracking solutions based on potentiometers or rotational encoders.

In this paper we investigate the use of body model constraints to improve the accuracy of inertial motion capture. The proposed method utilises the correlation between rotational motions and linear accelerations to estimate and correct for the corrupting effects of linear accelerations on accelerometer based orientation estimates. We demonstrate the positive effects of considering body model constraints on motion reconstruction accuracy and motivate a metric for assessing the quality of motion capture without reference to external sources of information.

The remainder of the paper is structured as follows. Section II presents a brief overview of inertial motion capture.

Section III presents an algorithm for combining the rotational parameters of sensors with body model constraints to estimate linear accelerations. Section IV discusses the simulation environment developed to test the behaviour of the algorithm. Section V presents the results of simulations to demonstrate the effectiveness of the algorithm, while Section VI presents a discussion of the results. Finally, Section VII presents the conclusions.

## II. INERTIAL MOTION CAPTURE OVERVIEW

Mapping of the orientations of inertial sensors to a body model composed of rigid bodies allows for reconstruction of the subject's posture [11]. Fifteen orientation sensing devices are sufficient to provide full body posture tracking [12], although more can be used to provide increased detail in areas such as the spine and shoulders.

The orientation of sensor devices is typically calculated by fusing inertial estimates, from rate gyroscope integration, with an absolute orientation reference, derived from observing the directions of the Earth's local gravitational and magnetic field vectors. Data fusion is achieved using either Kalman filter variants [8], [13], [14] or complementary filtering techniques [6], [10], [11]. The fusion of inertial estimates with an absolute reference allows for the use of relatively low-cost, low-accuracy, rate gyroscopes, as the inherent drift in orientation due to rate gyroscope bias can be counteracted.

There are numerous algorithms [15] for estimating orientation based on the observation of two, or more, non-collinear, non-zero vectors that are measured in the rotating co-ordinate frame of interest and known in a reference co-ordinate frame. These range from simple solutions, such as the TRIAD algorithm [16] that discards redundant data to guarantee a solution, to more complex algorithms, such as QUEST [17] that allow the contribution of each vector to be weighted based on its estimated accuracy.

All approaches to vector observation are limited in their accuracy by corruptions of the measured vectors that cause them to deviate from the expected reference. In the case of the magnetic field vector, corruption is due to the presence of ferrous materials in the capture environment. Attempts to minimise the resulting errors have been demonstrated [18].

The observation of the local gravity vector using a triaxial accelerometer is subject to corruption by linear accelerations

caused by subject motion. Existing methods to estimate and counteract this corruption [19] are based on estimating the dynamic kinematics of human motion to predict future linear accelerations from prior states. Such models are typically limited to modelling linear accelerations as coloured noise signals in the global reference frame.

### III. LINEAR ACCELERATION ESTIMATION ALGORITHM

We now consider the problem of estimating the linear accelerations of inertial sensors attached to a subject in order to improve the accuracy of vector observations and hence inertial motion capture. Rather than make assumptions about the dynamics of subject motion, we will investigate the correlation between rotational parameters and linear accelerations.

#### A. Correlation between rotational kinematics and linear accelerations

First consider the case of rigid body rotating about a point, fixed at the origin, at a constant angular velocity,  $\omega$ , measured in rad/s. Every point,  $P$ , on the body will experience a radial linear acceleration:

$${}^L\mathbf{l}_r = ({}^L\boldsymbol{\omega} \cdot {}^L\mathbf{o}) {}^L\boldsymbol{\omega} - {}^L\mathbf{o} \|{}^L\boldsymbol{\omega}\|^2 \text{ m/s}^2, \quad (1)$$

where  $\mathbf{o} = \overrightarrow{OP}$ , the offset of the point from the centre of rotation, in meters, and an  $L$  superscript indicates the local, inertial, co-ordinate frame.

Similarly, every point on a rigid body undergoing an angular acceleration,  $\alpha$ , measured in  $\text{rad/s}^2$ , will experience a tangential acceleration:

$${}^L\mathbf{l}_t = {}^L\boldsymbol{\alpha} \times {}^L\mathbf{o} \text{ m/s}^2. \quad (2)$$

Finally, consider the case where the body, rather than being in a stationary co-ordinate frame, is rotating about a point in a co-ordinate frame that is itself undergoing a linear acceleration. In this case all points in the accelerating frame will experience a uniform linear acceleration,  ${}^L\mathbf{l}_f \text{ m/s}^2$ .

The total linear acceleration of a point on a rotating rigid body under such circumstances is therefore:

$${}^L\mathbf{l} = {}^L\mathbf{l}_f + {}^L\mathbf{l}_r + {}^L\mathbf{l}_t \text{ m/s}^2. \quad (3)$$

#### B. Body model structure

We now consider the application of the equations presented in Section III-A to the idealised body model structure illustrated in Figure 1.

The model representing the subject's body is constructed from a tree of joints,  $J_k$ . Each joint can have zero or more child joints, where each child joint is offset from the parent by an offset,  $\mathbf{o}_{J_k}$ , specified in the parent's local co-ordinate frame. Joints are considered to be spherical, i.e. they rotate about a single point, while joint and sensor offsets are considered constant. The effect of these simplifications will be discussed further in section VI. The root of the body model tree, designated  $J_0$ , is taken to be the pelvis, as this is common practice in the computer animation field.

The rotation of each joint in the model is controlled by an associated inertial sensor. For the sake of simplicity it

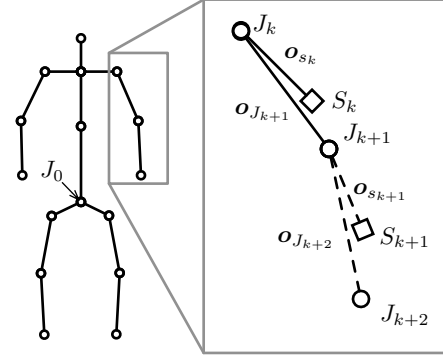


Fig. 1. Body model structure showing detail of sensor and joint offsets

---

#### Algorithm 1: Recursive function for estimating linear accelerations of sensors and joints

---

```

def estLinAccel(J)
    s = J.sensor
    /* Linear acceleration of sensor */
    {}^L\mathbf{l}_r = ({}^L\boldsymbol{\omega}_s \cdot {}^L\mathbf{o}_s) {}^L\boldsymbol{\omega}_s - {}^L\mathbf{o}_s \|{}^L\boldsymbol{\omega}_s\|^2
    {}^L\mathbf{l}_t = {}^L\boldsymbol{\alpha}_s \times {}^L\mathbf{o}_s
    {}^L\mathbf{l}_J = \hat{q}_s^* W \mathbf{l}_J \hat{q}_s
    {}^L\mathbf{l}_s = {}^L\mathbf{l}_J + {}^L\mathbf{l}_r + {}^L\mathbf{l}_t
    /* Estimate linear acceleration of
       child joints and recurse */
    for c in J.children :
        {}^L\mathbf{l}_r = ({}^L\boldsymbol{\omega}_s \cdot {}^L\mathbf{o}_c) {}^L\boldsymbol{\omega}_s - {}^L\mathbf{o}_c \|{}^L\boldsymbol{\omega}_s\|^2
        {}^L\mathbf{l}_t = {}^L\boldsymbol{\alpha}_s \times {}^L\mathbf{o}_c
        W \mathbf{l}_c = W \mathbf{l}_J + \hat{q}_s ({}^L\mathbf{l}_r + {}^L\mathbf{l}_t) \hat{q}_s^*
        estLinAccel(c)

```

---

is assumed that joints and sensors share a local inertial co-ordinate frame, with the rotation of the frame, relative to a global world co-ordinate frame, specified by the quaternion,  $q_{J_k}$ . This restriction can easily be removed but complicates the maths as an additional co-ordinate frame must be tracked.

Using the equations presented in Section III-A the linear acceleration of each joint, and associated sensor, can be calculated using Algorithm 1. The algorithm performs a pre-order traversal of the body model starting from the root joint.

For each joint the linear acceleration of the associated sensor is first calculated based on its rotational parameters and offset from the parent joint. The resulting linear acceleration is added to the linear acceleration of the parent joint to calculate the total acceleration. The linear accelerations of the child joints are calculated in a similar manner to that of the sensors.

The linear acceleration of joints are assumed to be in global world co-ordinates, designated by a superscript  $W$ , and are converted to local co-ordinates using the estimated sensor rotation,  $\hat{q}_s$ . Specifying the linear acceleration of the joint in world co-ordinates allows linear accelerations to be passed between joints in the shared global co-ordinate frame, reducing the amount of information that must be shared between joints.

Reducing the amount of shared data is important as it allows implementation of the algorithm to be distributed between IMUs for real time processing.

The root joint represents a special case as it has no parent to estimate its linear acceleration. This issue will be addressed further in Section IV-A.

#### IV. SIMULATION ENVIRONMENT

In order to test the behaviour of the linear acceleration estimation algorithm a simulation environment was developed that allows inertial sensor data to be generated from existing motion capture data. Use of simulated data allows a wide variety of motions to be tested and sources of error to be gradually introduced to assess their significance.

The simulation environment used for this paper, written in Python, allows motion data in BVH format to be mapped to a jointed body model as described in Section III-B. From the root position and relative orientation data in the BVH file the positions, velocities, accelerations, orientations, angular velocities, and angular accelerations of each model joint and sensor can be calculated.

Source motions for testing algorithm performance were taken from the Carnegie Mellon University motion capture database.<sup>1</sup> In order to reduce processing times, and simplify result presentation, source motion files in ASF/AMC format were pre-processed in Autodesk MotionBuilder to remove the upper body leaving the pelvis (root), and the left and right femur, tibia, foot and toes. The resulting body model was exported in BVH format. A direct method of importing motion data from ASF/AMC format is not currently supported, however, it only requires a new parser to be written.

Motion data was filtered using a low-pass filter with a cutoff at 18Hz to remove high frequency noise from the optical data that would otherwise dominate numerical estimates of derivative functions. After filtering of position and orientation data the derivative parameters were estimated using central difference approximations. The requirement to process data in this manner is a major disadvantage of using simulations driven by optical motion data. The filtering process is liable to remove true variations in measured parameters but is necessary to allow for reasonable approximations of derivative functions.

After importing motion data virtual orientation sensors were attached to the model. The sensor attached to the pelvis was collocated with the joint, while all other sensors were mapped on to the bone halfway between the proximal and distal joints, e.g. the right femur sensor was located halfway between the hip and knee.

Two captures were selected for examination in simulation. These were:

16\_15 470 frames; three walking gait cycles.

16\_55 180 frames; two running gait cycles.

All captures were sampled at 120Hz. The short duration of the motion capture data files presents a problem for simulation as it prevents analysis of the stability of orientation estimates over

---

#### Algorithm 2: Base complementary filter structured

---

```

def updateOrientation(a, m, ω)
  /* Inertial update */
   $\dot{\hat{q}} = \frac{1}{2}\omega\hat{q}_{t-1}$ 
   $\hat{q}_t = \hat{q}_{t-1} + \dot{\hat{q}}\Delta t$ 
  /* Estimate gravity vector */
   $\hat{g} = -(\mathbf{a} - \text{linAccelEst}(\dots))$ 
  /* Calculate vector observation */
   $q_{vo} = \text{QUEST}(\hat{g}, \mathbf{m})$ 
  if  $q_{vo} \cdot \hat{q} < 0$  then
    /* Resolve  $q \equiv -q$  ambiguity */
     $q_{vo} = -q_{vo}$ 
  end
  /* Apply drift correction */
   $\hat{q} = \hat{q} + \frac{1}{k}(q_{vo} - \hat{q}_t)$ 
   $\hat{q} = \hat{q} / \|\hat{q}\|$ 

```

---

long periods. This problem is common to the capture of gait motions as optical systems tend to have very limited capture volumes.

#### A. Filter implementations

The orientations of simulated sensors were estimated using a complementary filter structure proposed by Bachmann [11], outlined in Algorithm 2. Four filters were implemented, varying in their approach to estimating linear accelerations. The four approaches were:

Pure

The pure complementary filter without any linear acceleration estimation.

Local

The linear acceleration of sensors was estimated based on its previous estimate and the prediction model from Luinge et al. [19]:

$${}^W\hat{\mathbf{l}}_t^- = c \cdot {}^W\hat{\mathbf{l}}_{t-1} + \mathbf{w}, \quad (4)$$

where  $c$  is a constant and  $\mathbf{w}$  is a random noise source. The equation models the linear acceleration of a sensor in the global frame as a coloured noise signal shaped by a first order filter with a cutoff defined by  $c$ . The value of  $c$  was selected to match the 18Hz frequency filter applied to the motion capture data. After each update of the filter state the linear acceleration for the current sample was re-evaluated by subtracting the estimated gravity vector from the acceleration signal:

$${}^W\hat{\mathbf{l}}_t = \hat{q}^L \mathbf{a}_t \hat{q}^* - {}^W\mathbf{g}, \quad (5)$$

where  $\mathbf{g}$  is the reference gravity vector.

Perfect

The linear accelerations of sensors estimated using Algorithm 1. The algorithm was split into two phases: first, the linear acceleration of the sensor was

<sup>1</sup>Data available from mocap.cs.cmu.edu

TABLE I  
SIMULATED SENSOR NOISE PARAMETERS.

Sensor	Noise $\sigma$	Noise bandwidth
Accelerometers	0.3 m/s <sup>2</sup>	60Hz
Magnetometers	0.0003 %Full scale	60Hz
Rate Gyroscopes	0.03125 rad/s	60Hz

estimated and used to update the orientation estimate; second, the updated orientation was used to estimate the linear accelerations of child joints in the world frame.

The angular accelerations of the sensors were estimated by numerical differentiation of rotational rate data to simulate the behaviour of an IMU.

The linear acceleration of the root joint was taken directly from the true linear acceleration derived from the sensor position data.

#### Hybrid

As with the Perfect implementation the linear accelerations were estimated using Algorithm 1. The linear acceleration of the root joint was estimated using the dynamic model of the Local implementation.

In all filters the co-efficient,  $k$ , that controls blending between the inertial and vector observation estimates, was set to 64. This value was selected to provide a tradeoff between noise suppression and filter stability. Vector observation was performed using the QUEST algorithm, with equal weighting applied to the gravitational and magnetic field vectors.

#### B. Simulation details

Linear accelerations, angular velocities and angular accelerations were calculated by numerically differentiating position and rotation data. The simulated magnetic field vector was generated by rotating a reference magnetic field vector into the sensor local frame by means of the true sensor rotation. The simulations do not account for the effects of varying magnetic field inclination, instead assuming that the magnetic field vector is purely horizontal to the Earth's surface.

Simulations were performed with sensor data corrupted by gaussian coloured noise. The standard deviation of the sensor noise sources was estimated based on measurements performed on an IMU prototype. The noise was processed by a second order low-pass Butterworth filter, with a cutoff at 60Hz, to model the effect of an analogue anti-aliasing filter. The standard deviations of the sensor noise sources are given in Table I.

In addition to sensor noise the effects of rate gyroscope bias were modelled. Gyroscope bias was modelled as a constant offset normally distributed in each gyroscope axis with standard deviation of 0.03125 rad/s.

Monte Carlo simulation, with 1000 independent trials for each filter implementation, was used to assess the performance of the filters in the face of sensor noise and rate gyroscope bias. In each simulation run the initial orientations of the simulated sensors was initialised to the true orientation of the joint.

TABLE II  
MEAN RMS ERROR ANGLE (DEGREES) BETWEEN TRUE AND ESTIMATED SENSOR ORIENTATIONS. WALKING GAIT.

Joint	Pure	Local	Perfect	Hybrid	RMS $\ L\ $ m/s <sup>2</sup>
pelvis	1.56	0.98	0.54	1.30	3.7
rfemur	3.07	2.10	0.69	1.20	6.3
rtibia	4.39	2.93	0.87	1.34	11.1
rfoot	6.93	4.53	1.19	1.58	17.1
rtoes	7.79	4.71	1.57	1.89	20.9
lfemur	2.81	2.06	0.68	1.21	5.8
ltibia	3.96	2.84	0.78	1.28	10.5
lfoot	5.41	4.17	1.21	1.58	15.1
ltoes	5.19	4.65	1.32	1.68	18.1

TABLE III  
 $r^2$  CO-EFFICIENT OF DETERMINATION BETWEEN TRUE SENSOR ACCELERATION AND ACCELERATION ESTIMATE. WALKING GAIT.

Joint	Local			Hybrid		
	$x$	$y$	$z$	$x$	$y$	$z$
pelvis	0.728	0.705	0.725	0.939	0.929	0.987
rfemur	0.823	0.568	0.677	0.981	0.994	0.997
rtibia	0.842	0.580	0.775	1.000	1.000	0.999
rfoot	0.885	0.588	0.876	0.986	0.996	0.997
rtoes	0.882	0.600	0.836	0.991	0.997	0.998
lfemur	0.811	0.543	0.686	0.988	0.995	0.998
ltibia	0.817	0.553	0.751	0.997	0.996	0.999
lfoot	0.860	0.557	0.846	0.999	0.996	0.998
ltoes	0.850	0.573	0.803	0.999	0.996	0.998

## V. RESULTS

The accuracy of the four different orientation filter implementations are summarised in Table II, for the walking trial, and Table IV, for the running trial. The tables show the mean RMS error angle for each joint in the body model. The error angle,  $\theta$ , was calculated at each sample as the angle between the true joint rotation,  $q$ , and the rotation estimated by the orientation filter,  $\hat{q}$ :

$$\theta = 2 \arccos((q \otimes \hat{q}^*)_w). \quad (6)$$

In addition to the error angles, the tables show the RMS magnitude of the linear acceleration experienced by the sensor attached to each joint.

The results for the walking trial, Table II, show that the pure complementary filter has the worst performance. The magnitude of the orientation error is related to the magnitude of the linear acceleration experienced by the sensor. Larger linear accelerations result in greater potential corruption of the observed gravitational field vector and hence greater orientation errors.

The local linear acceleration estimation approach results in a small increase in orientation accuracy. The ability of the local linear acceleration estimation algorithm to predict future linear accelerations is illustrated in Table III. The results indicate that there are substantial linear accelerations not predicted by the simple dynamic model. It is possible, however, that a different choice of filter co-efficient,  $c$ , would result in improved performance.

The perfect model based approach results in the lowest orientation error angle. However, as this model is not practically realisable, due to the assumption of prior knowledge of

TABLE IV  
MEAN RMS ERROR ANGLE (DEGREES) BETWEEN TRUE AND ESTIMATED  
SENSOR ORIENTATIONS. RUNNING GAIT.

Joint	Pure	Local	Perfect	Hybrid	RMS $\ \hat{l}\ $ m/s <sup>2</sup>
pelvis	5.07	2.98	0.72	0.86	11.9
rfemur	5.99	4.75	1.43	1.48	20.5
rtibia	6.72	5.31	1.50	1.55	37.6
rfoot	9.32	7.46	1.87	1.91	54.7
rtoes	11.17	8.12	2.53	2.56	61.3
lfemur	9.15	6.17	1.50	1.55	16.9
ltibia	6.24	4.51	1.52	1.57	35.5
lfoot	8.04	5.87	2.25	2.31	54.8
ltoes	8.27	6.64	2.91	2.95	62.4

TABLE V  
 $r^2$  CO-EFFICIENT OF DETERMINATION BETWEEN TRUE SENSOR  
ACCELERATION AND ACCELERATION ESTIMATE. RUNNING GAIT

Joint	Local			Hybrid		
	$x$	$y$	$z$	$x$	$y$	$z$
pelvis	0.790	0.798	0.795	0.939	0.990	0.999
rfemur	0.836	0.737	0.885	0.980	0.998	0.999
rtibia	0.875	0.789	0.757	0.995	0.997	0.976
rfoot	0.889	0.781	0.757	0.997	0.997	0.970
rtoes	0.896	0.773	0.773	0.998	0.996	0.973
lfemur	0.855	0.719	0.872	0.978	0.996	0.998
ltibia	0.883	0.791	0.826	0.997	0.999	0.987
lfoot	0.885	0.797	0.832	0.998	0.999	0.993
ltoes	0.889	0.801	0.819	0.998	0.999	0.992

the root joint's linear acceleration, it serves only as baseline for the accuracy of the hybrid model. The hybrid model shows similar performance to the perfect model. Both model based approaches perform substantially better than either the local or pure implementations. The reason for the improved performance of the hybrid model is its ability to predict accurately the linear accelerations experienced by orientation sensors, as illustrated in Table III.

The results of the running trial, presented in Table IV, show a similar tendency to the walking trial. The greater linear accelerations during the capture result in increased error for all filter implementations. As with the walking trial, the pure complementary filter performs the worst as it is unable to compensate for the effects of linear acceleration on vector observations.

The hybrid model based approach again results in more accurate linear acceleration estimation, as shown in Table V, which in turn results in improved error performance.

## VI. DISCUSSION

The results presented in Section V demonstrate that using body model constraints can improve the accuracy of inertial motion capture by accurately estimating and removing the effects of linear accelerations. While results have been presented from only two motions, and only for the lower body, the hybrid algorithm has been tested on a variety of full body motions with consistent results.

### A. Body model optimisation

The ability of the hybrid algorithm to estimate linear accelerations accurately relies on the accuracy of the underlying body model. The current body model, modelling all joints as

perfect spherical joints, is an idealisation of a true kinematic subject model. In practice the joints of a real subject are liable to be more complex. The result of these variations require further simulation to assess their effect on estimation accuracy. If necessary the kinematics of the specific joints could be modelled at the expense of increased algorithm complexity and loss of generality.

In addition to the knowledge of limb segment lengths and joint connectivity, required for reconstructing the posture from inertial sensor data, the new algorithm additionally requires knowledge of the sensor offsets. While the limb lengths may be expected to remain constant for a given subject, and thus only require a one time initialisation, the offsets of sensors are likely to vary for each capture depending on the attachment mechanism. It is therefore desirable to have a way of automatically estimating the sensor offsets.

To automate the process of estimating sensor offsets we first examine the expected outcome of the linear acceleration estimation algorithm. Under ideal circumstances the measured acceleration,  ${}^L\mathbf{a}$ , will equal the combination of the estimated linear acceleration,  ${}^L\hat{\mathbf{l}}$ , and the estimated gravity vector,  ${}^L\hat{\mathbf{g}} = \hat{\mathbf{q}}^* W \mathbf{g} \hat{\mathbf{q}}$ .

$${}^L\mathbf{a} = {}^L\mathbf{l} - {}^L\mathbf{g} = {}^L\hat{\mathbf{l}} - {}^L\hat{\mathbf{g}} \quad (7)$$

In practice, we would expect minor differences between the measured acceleration and the estimate due to sensor noise and numerical precision. Therefore we may restate (7) as:

$${}^L\mathbf{a} - {}^L\hat{\mathbf{l}} + {}^L\hat{\mathbf{g}} = \mathbf{r}, \quad (8)$$

where  $\mathbf{r}$  is a residual error vector. As under ideal conditions  $\mathbf{r} = \mathbf{0}$ , we can seek to minimise the cost function:

$$C = \sum_{s=0}^S \sum_{n=0}^N \|\mathbf{r}_n\|, \quad (9)$$

where  $S$  is the number of samples in a trial capture, and  $N$  is the number of sensors. The sensor offsets can be determined using normal optimisation techniques provided that unprocessed sensor data is available for a capture with at least some linear acceleration present for every joint. This process would only need to be performed at the start of each capture session as the computed values could be stored for subsequent captures.

In order to determine the effect of offset errors, both in sensor positions and limb segment lengths, a further simulation was performed using the walking capture. The model was first processed, using the Hybrid sensor algorithm and the sensor noise parameters from Table I, to calculate the RMS error angles in the absence of offset errors.

A normally distributed offset, with standard deviation of 5 cm in each axis, was applied to each joint and sensor offset. The model was then reprocessed to calculate the RMS error angles caused by the corrupted offset values. The sensed data remained unchanged from the initial simulation.

Finally, the joint and sensor offsets were estimated by minimising the cost function, Equation 9, using the Levenberg-Marquardt *lmdif* algorithm from MINPACK [20]. The model

TABLE VI

RMS ERROR ANGLE(DEGREES) BETWEEN TRUE AND ESTIMATED SENSOR ORIENTATION WITH JOINT AND SENSOR OFFSET ERRORS.

Joint	Zero offset error	w/ Offset error	w/ Optimised offsets
root	1.64	1.63	1.64
rfemur	1.81	2.00	1.82
rtibia	1.78	2.07	1.81
rfoot	2.29	4.21	2.31
rtoes	2.65	6.08	2.78
lfemur	2.20	2.41	2.20
ltibia	2.00	3.30	2.02
lfoot	2.92	5.51	2.96
ltoes	2.32	5.32	2.31

TABLE VII

MAGNITUDE OF JOINT AND SENSOR OFFSET ERRORS BEFORE AND AFTER OPTIMISATION.

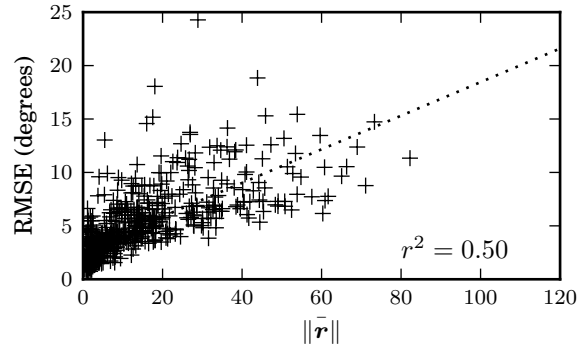
Joint	Joint offset (cm)		Sensor offset (cm)	
	Before	After	Before	After
root	na	na	8.8	0.0
rfemur	5.9	0.5	7.3	0.8
rtibia	10.9	1.3	9.0	0.5
rfoot	5.5	0.9	13.1	0.2
rtoes	15.6	0.9	12.5	0.8
lfemur	17.8	0.4	3.5	0.6
ltibia	10.1	1.4	9.1	0.7
lfoot	5.4	1.4	7.6	0.2
ltoes	3.7	0.7	13.4	0.3

was reprocessed once more to generate the RMS error angles with the optimised offsets.

The results of the simulation are displayed in Tables VI and VII. From Table VI it is clear that offset errors result in degraded orientation accuracy, as we would expect given that offset errors result in reduced ability to compensate for linear accelerations. Table VII indicates that minimising the cost function results in substantially reduced offset errors. These reduced offset errors result in similar performance to the original perfect information.

The standard deviation of offset errors was deliberately chosen to be larger than that which might be expected given careful measurement of the subject body model and sensor positions. This was done to ensure that the optimisation was convergent even in the event of relatively large errors. Convergence of the optimisation process was confirmed over multiple independent simulations.

In order to perform optimisation of joint and sensor offsets in an efficient manner it is useful to take advantage of the structure of the body model. A naive approach to minimising (9) would be to attempt to optimise all offsets at once. For the lower body model used in this paper this would require optimising fifty-one parameters. The alternative method, used in this paper, is to optimise one joint at a time starting from the root. This reduces the number of parameters to optimise at a time to a more manageable six. Additionally the process may be parallelised wherever the body model tree structure splits, allowing for a significant improvement in convergence time. Further work is required to investigate the number of samples, and the qualitative properties of the motion, required to minimise the optimisation time.

Fig. 2. Linear regression of  $\|\bar{\mathbf{r}}\|$  and RMSE error angle

### B. Orientation accuracy metric

Equation 8 also suggests a metric for assessing the quality of orientation estimation without reference to an external truth reference such as optical data. The ability of a device to estimate its expected gravity vector accurately is dependent on the orientation accuracy, while its ability to estimate its linear acceleration, dependent on the accuracy of the estimation model, will affect subsequent orientation estimates. Therefore, we would expect that the mean residual error between the measured acceleration and the acceleration estimated by the IMU will be strongly related to the accuracy of the orientation estimates. A low mean residual error would indicate that the IMU was accurately tracking its orientation. Furthermore, when using the hybrid linear acceleration model, a low mean residual error value would indicate a good fit between the body model and reality.

To test the hypothesis that the mean residual error provides a reasonable predictor of error, the pure, local, and hybrid estimation algorithms were simulated on the entire set of full body captures from subject 16 of the CMU corpus. The resulting RMS errors were plotted against the mean residual error for each joint, as shown in Figure 2. A simple linear regression was performed to test the prediction value of the mean residual error metric. The moderate resulting co-efficient of determination indicates that the mean residual error is not capable of directly predicting RMS error. However, there is a reasonable level of correlation.

## VII. CONCLUSION

A method for estimating the linear acceleration of IMUs based on subject body model constraints has been demonstrated, through simulation, to be capable of estimating linear accelerations with a high degree of accuracy. The resulting linear acceleration estimates allow for greater accuracy of orientation estimates compared to existing solutions.

The proposed method requires that, in addition to the body model required for posture reconstruction, the offsets between sensors and associated joints be known. A cost function for automated optimisation of sensor offsets has been proposed based on minimising the residual errors between measured

and estimated accelerations. Use of this cost function allows both joint and sensor offsets to be estimated in a least-squares optimal manner. Finally, a metric for quantifying the quality of inertial motion capture has been proposed based on the mean residual error. The metric is unable to account for the full variation in RMS error but does indicate a significant correlation. Further work is required to investigate the use of the residual error function, both as a cost function for model optimisation and as a metric for capture accuracy.

#### ACKNOWLEDGEMENTS

This work was supported by the UK Engineering and Physical Sciences Research Council under the Basic Technology Research Programme, Grant C523881 entitled “Research Consortium in Speckled Computing”. The optical motion data used in this project was obtained from mocap.cs.cmu.edu. The database was created with funding from NSF EIA-0196217.

#### REFERENCES

- [1] R. Aylward, S. D. Lovell, and J. A. Paradiso, “A compact, wireless, wearable sensor network for interactive dance ensembles,” in *Wearable and Implantable Body Sensor Networks, International Workshop on*, 2006, pp. 4 pp.–.
- [2] A. Lynch, B. Majeed, J. Barton, F. Murphy, K. Delaney, and S. O’Mathuna, “A wireless inertial measurement system (WIMS) for an interactive dance environment,” *Journal of Physics: Conference Series*, vol. 15, pp. 95–100, 2005.
- [3] C. Park, P. H. Chou, and Y. Sun, “A wearable wireless sensor platform for interactive dance performances,” in *Pervasive Computing and Communications, Fourth Annual IEEE International Conference on*, 2006, pp. 52–59.
- [4] Q. Li, J. Stankovic, M. Hanson, A. Barth, J. Lach, and G. Zhou, “Accurate, fast fall detection using gyroscopes and accelerometer-derived posture information,” in *Wearable and Implantable Body Sensor Networks, Proceedings of the International Workshop on*, vol. 9, 2009, pp. 138–143.
- [5] K. Lorincz, B.-r. Chen, G. W. Challen, A. R. Chowdhury, S. Patel, P. Bonato, and M. Welsh, “Mercury: a wearable sensor network platform for high-fidelity motion analysis,” in *Embedded Networked Sensor Systems, Proceedings of the 7th ACM Conference on*, 2009, pp. 183–196.
- [6] V. van Acht, E. Bongers, N. Lambert, and R. Verberne, “Miniature wireless inertial sensor for measuring human motions,” in *Engineering in Medicine and Biology Society, Proceedings of the 29th Annual International Conference of the IEEE on*, Aug. 2007, pp. 6278–6281.
- [7] F. Brunetti, J. Moreno, A. Ruiz, E. Rocon, and J. Pons, “A new platform based on IEEE802.15.4 wireless inertial sensors for motion caption and assessment,” in *Engineering in Medicine and Biology Society, Proceedings of the 28th IEEE Annual International Conference on*, 2006.
- [8] H. J. Luinge, P. H. Veltink, and C. T. M. Baten, “Ambulatory measurement of arm orientation,” *Journal of Biomechanics*, vol. 40, no. 1, pp. 78–85, 2007.
- [9] W.-S. Yeoh, J.-K. Wu, I. Pek, Y.-H. Yong, X. Chen, and A. B. Waluyo, “Real-time tracking of flexion angle by using wearable accelerometer sensors,” *Medical Devices and Biosensors, 5th International Summer School and Symposium on*, pp. 125–128, June 2008.
- [10] A. Young, M. Ling, and D. K. Arvind, “Orient-2: A realtime wireless posture tracking system using local orientation estimation,” in *Embedded networked sensors, Proceedings of the 4th workshop on*, 2007, pp. 53–57.
- [11] E. R. Bachmann, “Inertial and magnetic tracking of limb segment orientation for inserting humans into synthetic environments,” Ph.D. dissertation, Naval Postgraduate School, Monterey, California, 2000.
- [12] R. Zhu and Z. Zhou, “A real-time articulated human motion tracking using tri-axis inertial/magnetic sensors package,” in *Neural Systems and Rehabilitation Engineering, IEEE Transactions on*, vol. 12, no. 2, June 2004, pp. 295–302.
- [13] X. Yun and E. R. Bachmann, “Design, implementation, and experimental results of a quaternion-based Kalman filter for human body motion tracking,” *Robotics, IEEE Transactions on*, vol. 22, no. 6, pp. 1216–1227, 2006.
- [14] J. Torres, B. O’Flynn, P. Angove, F. Murphy, and C. O. Mathuna, “Motion tracking algorithms for inertial measurement,” in *Body area networks, Proceedings of the ICST 2nd international conference on*, 2007, pp. 1–8.
- [15] F. Markley and D. Mortari, “Quaternion attitude estimation using vector observations,” *Journal of the Astronautical Sciences*, vol. 48, no. 2, pp. 359–380, 2000.
- [16] G. Lerner, *Spacecraft Attitude Determination and Control*. Kluwer Academic Pub, 1978, ch. Three-Axis Attitude Determination, pp. 420–428.
- [17] M. Shuster and S. Oh, “Three-axis attitude determination from vector observations,” *Journal of Guidance and Control*, vol. 4, no. 1, pp. 70–77, 1981.
- [18] D. Roetenberg, “Inertial and magnetic sensing of human motion,” Ph.D. dissertation, Universiteit Twente, 2006.
- [19] H. Luinge and P. Veltink, “Measuring orientation of human body segments using miniature gyroscopes and accelerometers,” *Medical and Biological Engineering and Computing*, vol. 43, no. 2, pp. 273–282, 04 2005.
- [20] J. Moré, D. Sorenson, B. Garbow, and K. Hillstrom, “The MINPACK project,” *Sources and Development of Mathematical Software*, pp. 88–111, 1984.